MATERIALS SCIENCE

Quick liquid packaging: Encasing water silhouettes by three-dimensional polymer membranes

Sara Coppola[1]*, Giuseppe Nasti[1], Veronica Vespini[1], Laura Mecozzi[1], Rachele Castaldo[2], Gennaro Gentile[2], Maurizio Ventre[3], Paolo A. Netti[3,4], Pietro Ferraro[1]*

One of the most important substances on Earth is water. It is an essential medium for living microorganisms and for many technological and industrial processes. Confining water in an enclosed compartment without manipulating it or by using rigid containers can be very attractive, even more if the container is biocompatible and biodegradable. Here, we propose a water-based bottom-up approach for facile encasing of short-lived water silhouettes by a custom-made adaptive suit. A biocompatible polymer self-assembling with unprecedented degree of freedom over the water surface directly produces a thin membrane. The polymer film could be the external container of a liquid core or a free-standing layer with personalized design. The membranes produced have been characterized in terms of physical properties, morphology and proposed for various applications from nano- to macroscale. The process appears not to harm cells and microorganisms, opening the way to a breakthrough approach for organ-on-chip and lab-in-a-drop experiments.

INTRODUCTION

The possibility of isolating, engineering, and shaping materials into two-dimensional (2D) or 3D objects from the nanometer to the millimeter scale is a field of research that is constantly gaining importance. The problems of object isolation from a reactive environment and understanding the physics and chemistry of surface passivation are of great importance for a variety of applications such as microelectronics, drug delivery, forensics, archeology/paleontology, and space research (*1*–*3*). The isolation could be important for the physiochemical protection of objects from the reactive environment or to protect this from toxic or radioactive nature of the isolated object (*4*). Considerable efforts were made to control the material morphological properties a priori. Different technological methods of microfabrication including two-photon polymerization, soft interference lithography, replica molding, and self-folding polymers have been widely used for shaping and isolating the material of interest (*5*–*9*). Unfortunately, chemical-physical pretreatments are often required to gain the desired final properties, thus protracting the preparation time before and after the fabrication process. However, having a novel method for coating 2D or 3D objects in a single step would represent, in the microengineered field, a highly promising tool for biomaterials and tissue engineering, optics, and photovoltaic and nano-microelectronics devices (*10*–*12*). Concerning the biomaterials field, it is of great interest the investigation of cellular behavior of cells in complex 3D matrices, which mimic the multiscale arrangements of the native extracellular matrix (*13*). This could help unravel the mechanisms underpinning cell-material interactions for guiding stem cell fate and functions and characterize cancer cell behavior and tumor progression (*14*). In addition, matrices with complex structures can potentially provide useful hints for the development of organ-on-chip and drug testing devices (*15*). Moreover, encapsulating polymer coatings around objects could be mechanically robust, chemically protective, and yet highly transparent to electrons and photons in a wide energy range, thus enabling microscopic and spectroscopic access to encapsulated objects (*16*).

Interfacial phenomena occurring at the air-liquid or liquid-liquid interface have been extensively used in the last decades to create shells of orderly assembled nanoparticles or crystals or to create micro- and nanostructured polymeric membranes (*17*). This is in contrast to the conventional techniques involving the use of solid molds to create micro- and nanopatterned material surfaces. Therefore, surface tension may potentially be used to sculpt synthetic structures, and a sapient modulation of such tensions might, in principle, allow us to use liquids as molds for a rapid and versatile fabrication of complex material surfaces. Recently, a new method for controlling the surface tension and the capillarity as driving forces for the formation of liquid nanofluidic instabilities and polymer shapes has been proposed (*18*–*21*). In particular, this method is able to control the shape of unsteady polymeric structures by an electrohydrodynamic pressure to cure them by appropriate thermal treatments, finalizing them for photonic application and biomedical devices. Likewise, a simple method based on water casting has been proposed for the fabrication of ultrathin polymeric film, but there is still a running unsatisfied interest in smart tools for the production of 3D shapes (*22*). Very recently, direct solid wrapping of liquids with ultrathin sheets was developed with the aim of creating 3D shapes by tailoring the 2D boundary of a polymer film (*23*). In addition, the formation of a liquid-core capsule having a thin hydrogel membrane has been pursued by phase transition in the case of water and oil core (*24*). Until now, the major drawback is that the fabrication of the polymeric membrane is the consequence of a polymeric drop immersed in water, so that it is not possible to produce free-standing polymeric suites. We start from this approach envisaging the opportunity of broadening the polymer wrapping of liquid to the wrapping of inorganic and organic micro-objects or microstructured surfaces, removing the liquid core required for the fabrication.

[1]Institute of Applied Sciences and Intelligent Systems "E. Caianiello," Via Campi Flegrei 34, 80078 Pozzuoli, Italy. [2]Institute for Polymers, Composites and Biomaterials, CNR, Via Campi Flegrei 34, 80078 Pozzuoli, Italy. [3]Department of Chemical, Materials and Industrial Production Engineering, University of Naples Federico II, Piazzale Tecchio 80, 80125 Naples, Italy. [4]Center for Advanced Biomaterials For Healthcare @CRIB, Istituto Italiano di Tecnologia, Largo Barsanti e Matteucci 53, 80125 Naples, Italy.
*Corresponding author. Email: s.coppola@isasi.cnr.it (S.C.); pietro.ferraro@cnr.it (P.F.)

Here, we propose a water-based bottom-up approach for the straightforward shaping of polymer membranes and encapsulation of microbodies on arbitrary substrates. The process comprises the self-assembly of a biocompatible polymer over water surface, and it is characterized by an unprecedented versatility in enabling the formation of membranes of complex shapes in a fast and consistent manner. Being a liquid, water can take flexible forms assuming the shape of its container, and as a direct result, the self-assembled encapsulation membrane that we propose wraps in different geometries, generating a thin polymer film following the existing water profile and eventually sealing all the elements included in the water. Poly (lactic-*co*-glycolic acid) (PLGA) was chosen owing to its tunable structure, drug release efficiency, and high biosafety and biocompatibility. It is considered one of the most exploited, yet promising materials for application in biology and biomedicine (*25*). The polymer film could be the external container of a liquid core or could be a free-standing membrane with various designs. The obtained membranes have been characterized in terms of physical properties and morphology. In particular, the proposed technique inducing membrane self-assembly on aqueous solution or water-rich environments can be implemented over diverse spatial configurations, such as micropillars, organic and inorganic micro-objects, and colloidal particles, under mild conditions allowing the membranes to form in the presence of cells or microorganisms.

RESULTS

Polymer packaging on water surface

Once a droplet of a biocompatible polymeric solution, i.e., PLGA dissolved in dimethyl carbonate (DMC), is placed on a water surface, it forms a nonporous film instantaneously. Such a process shares similarities with the spontaneous film formation technique (*26*). In particular, as soon as a small polymer solution droplet is juxtaposed to and comes in contact with a water droplet standing on a hydrophobic surface, the polymer solution wraps the free water surface and starts to creep on the top of the droplet (see movie S1). The driving force for this mechanism is the reduction of the surface tension of water; i.e., the system goes to a state of lower energy converting the water-air interface into water–polymer solution and air–polymer solution interfaces. As the creation of a new surface requires energy, the energetic gain due to surface tension reduction compensates the creation of a new interface (Fig. 1A, left). At this point, the DMC solvent is extracted by water, and the surface tension acts as a driving force. Provided that the viscosity of the solution remains sufficiently low and fostered by the low volatility of DMC and slow solvent extraction by the aqueous phase, PLGA spreads over the water surface accommodating its contours (Fig. 1A, right). Because of the slow solvent extraction process, phase separation within the polymer solution does not occur, thus generating a homogeneous, nonporous film (*27*). This process usually takes a few seconds to occur. Of course, a small DMC evaporation should be expected, but the dominant factor in this is the solvent extraction in water. By performing an analogous experiment in which the polymer solution is juxtaposed to a DMC-saturated water droplet [13.9% (w/v)], we did not observe the rapid formation of a solid shell, but polymer solidifies over a longer time scale (i.e., minutes).

The polymer film thus produced extends all over the free aqueous surface, acquiring the shape and the structure of the liquid used as a 2D or 3D template. By controlling the volume of the dispensed solution, the amount of polymer, and the nonsolvent surface area, it is possible to control the film thickness. The fabrication process was tested on different liquids such as cell culture medium, phosphate-buffered saline (PBS), protein/peptide, and other buffer solutions having water as a component. A polymer film is created even in the case of dynamic and unstable conditions as in the case of a drop standing over a glass slide (Fig. 1B) and a drop flowing out of a needle (Fig. 1C). In the case of a stable liquid bridge between two plates, the polymer drop is just pipetted over the convex wall, and the membrane spreads all over the surface embracing the entire liquid structure (see Fig. 1D). The film is immediately formed once the solution drop comes into contact with the water, and the solvent evaporates so that when the water is dried off, the polymer maintains the 3D structure

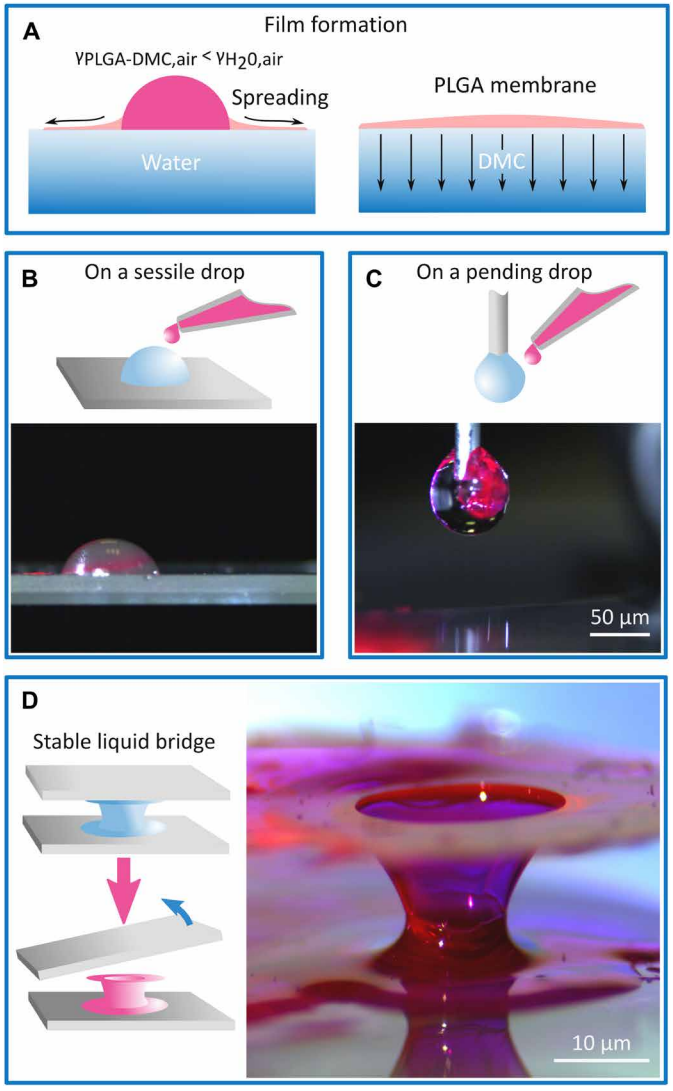

Fig. 1. Polymer packaging on water surface. (**A**) The mechanism for the formation of the PLGA membrane is composed of a phase of polymer solution spreading by surface tension over the free water surface while the DMC solvent diffuses, leading to the solidification of the PLGA membrane. Water packaging methods are shown in stable/static and dynamic/unstable conditions: (**B**) on a sessile drop on hydrophobic substrate and (**C**) wrapping, in real time, a drop flowing out of a needle. (**D**) Explanation of the 3D packaging approach over the wall of a stable liquid bridge between two plates.

acquired from the hosting liquid as shown in Fig. 1D. Under this condition, the film has no time to collapse under the atmospheric pressure. In this case, the membrane acts as a sort of external coating similar to a polymeric shell directly developed over the liquid drop in a noncontact mode. To demonstrate the total encasing of the liquid volume, we formed two separate sessile droplets on a Teflon slide, where only one was encased by the membrane (see movie S2). Tilting the substrate, the free water droplet moved along the substrate and then, once it arrived at the edge, fell down. Instead, the sessile drop coated with the membrane remained irremovable, since the membrane completely encloses and leaves it anchored to the glass substrate.

Membrane characterization

We used multiple techniques to characterize the morphological physical features of PLGA membranes obtained by liquid packaging (see Materials and Methods).

Scanning electron microscopy (SEM) images (Fig. 2, A and B) revealed a nonporous and symmetric structure of the membrane that is characterized by a homogeneous surface and thickness. The surface roughness is negligible at the micrometric scale, and nanometric irregularities are only observed at high magnifications (Fig. 2B). The membrane thickness, calculated by SEM observation, is 1.65 ± 0.05 μm. We performed static measurements of the water contact angle (CA) on the membrane, as reported in Fig. 2C. We found an average CA value of 73° ± 1°, typical of mildly hydrophilic polymers. Compared to conventional films of polylactic acid (PLA), the water CA of PLGA is lower because of the presence of the less hydrophobic glycolic acid segments in comparison to the lactic acid ones (*28*–*30*). Moreover, the membrane showed a good transparency to visible light, with a transmittance above 90% in the wavelength range from 250 to 800 nm (Fig. 2D) and an adsorption peak centered at 208 nm. We investigated mechanical properties of the PLGA membrane by tensile tests performed on a microtensile stage. A typical stress-strain curve recorded on PLGA samples is reported in Fig. 2E. The Young's modulus of the membrane is 75 ± 1 MPa, and the yield stress is 5.3 ± 0.2 MPa. Yielding occurs at 10 ± 2% strain, after which the sample is deformed at almost constant stress up to about 30%. These values are consistent with data reported in literature for PLGA films by considering the different thickness and test conditions. More specifically, the Young's modulus obtained for the PLGA membranes was lower with respect to literature data because of the lower strain rate used in our experimental setup (*31*). Last, we investigated gas barrier properties of the PLGA membrane by measuring oxygen and water vapor permeability. The membrane showed high barrier properties to water vapor. The calculated water vapor permeability on the membrane was 140 ± 8 (g μm)/(m^2 day kPa), more than one order of magnitude lower than that reported for the PLA homopolymer (*32*). Moreover, the membrane shows a very high permeability to oxygen, this parameter is very interesting for biological and biomedical applications. The calculated oxygen permeability was $1.90 \times 10^5 \pm 0.12 \times 10^5$ (cm^3 μm)/(m^2 day atm), about one order of magnitude higher than the oxygen permeability of PLA (*33*, *34*). For the characterization, we focused on bulk samples consisting of flat membranes fabricated in a petri dish filled up with water. Adopting this approach, we were able to use multiple samples produced with the same protocol as described in Materials and Methods.

Furthermore, we investigated and reported the formation of the polymeric membrane also on a sessile liquid droplet at the microscale (diameter, ~200 μm). In this case, we observed in the central zone

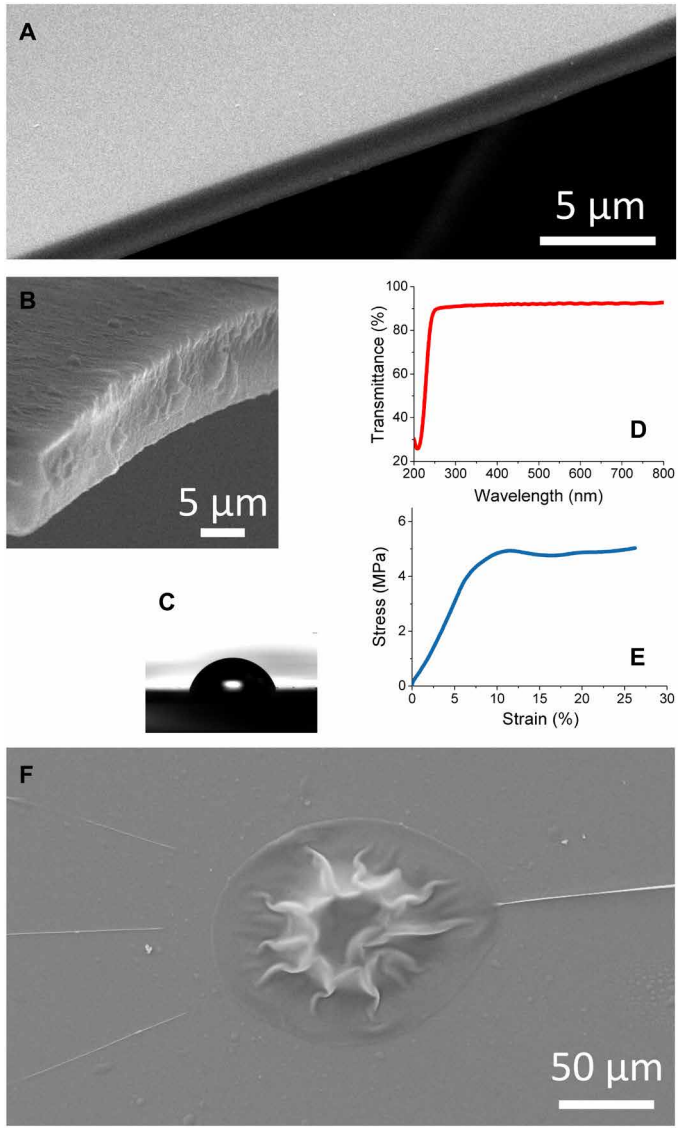

Fig. 2. Results of the PLGA membrane characterization. SEM images of the PLGA membrane (**A** and **B**), water CA (**C**), ultraviolet (UV)–visible spectrum (**D**), and stress-strain curve (**E**). (**F**) SEM image of a collapsed membrane on microscale sessile drop.

corresponding to the apex of the liquid droplet a collapsed and wrinkled membrane formed under the evaporation process of water obtained at RT for 3 weeks (Fig. 2F). The formation of wrinkles during this period is guided by the change in time of the volume accompanied by the drying of the underlying droplet. The remaining surrounding membrane morphology appears quite uniform, showing a complete wrapping and spreading on the supporting substrate as suggested by the symmetry of the collapsed membrane and the lack of holes, defects, and seams. Additional experiments on the complete wrapping and the membrane morphology in the case of uneven and 3D substrate are reported in the Supplementary Text 1 and figs. S1 to S3.

Biocompatible coating over a lab-in-a-drop system containing living organisms

One of the major advantages related to biopolymer manipulation with the proposed technique lies in the versatility of the process,

thus resulting in a high adaptability of the microstructure produced that is able to retrace complex contours of water-rich media. In particular, the straightforward self-assembling of a biopolymer into free-standing polymer sheets for the packaging of macro- and microstructures embedded in a water drop would be a unique aspect of our method. From the perspective of applying the process in the biomedical field, it is crucial to ensure the viability of biological entities present in the aqueous-rich template during membrane formation. For example, the process can, in principle, be used as an external coating for lab-in-a-drop experiments, paving the way to new methods for real-time observation in a 3D context. To prove these potentialities, we studied the behavior of *Caenorhabditis elegans*, a consolidated model organism for the study of neuron systems (*35*, *36*), during the process of packaging. In our experiments, *C. elegans* were placed in a water solution, and the water packaging technique was implemented by dispensing a polymer solution drop over the volume of interest to form a polymer membrane (the process was observed in real time through a charge-coupled device camera mounted over a Zeiss stereomicroscope). When the PLGA membrane wrapped around the liquid drop, the microorganisms immediately decreased their movement. In particular, they remained stretched in the direction parallel to the basal plate, passing from a condition of speed swimming to a sort of induced paralysis (see Fig. 3 and movie S3). *C. elegans* adhered to the water-PLGA membrane, and the oxygen flow was guaranteed by the permeability of the membrane. The change of behavior, although abrupt, was reversible. As soon as the membrane was removed, the microorganisms recovered their usual motility (see movie S4). Although investigating the causes that induced such a sharp change in behavior of the *C. elegans* is well outside the scope of this work, it is tempting to speculate that the paralysis was likely to be induced by the combination of two factors, i.e., the physical constrain of the membrane and the presence of DMC. Once the polymer membrane is formed, the *C. elegans* consequently reduce their normal pumping activity, avoiding the harmful side effects of the undesirable accumulation of drugs commonly used to reduce their speed for studying the lab-in-a-drop system. The membrane could be kept on the drop for all the time needed for the observation. The phenomenon proposed here is very interesting and will be examined in-depth in the future for real-time bioanalysis. Nevertheless, further experiments need to be performed to thoroughly understand the role of membrane formation on *C. elegans* behavior.

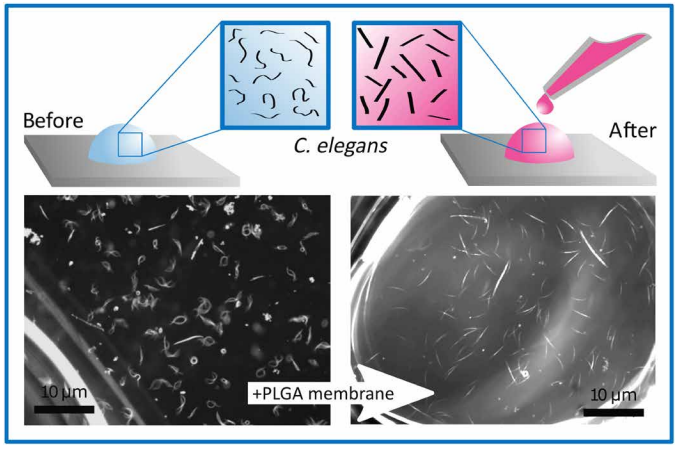

Fig. 3. Biocompatible coating over a lab-in-a-drop system containing living organisms. A drop of water with *C. elegans* swimming inside is shown (left). The PLGA membrane envelops the drop, inducing the momentary paralysis of the organisms. The process is even reversible: Peeling off the membrane keeps *C. elegans* moving as before.

Polymer packaging of micropillars, macroarray, and optical fiber

In the hypothesis that the driving force of the process is the reduction of the surface free energy with the interposition of a solid interface between the two liquid phases, we questioned whether this phenomenon could occur in the presence of complex contours or obstacles or even on hydrogels. Along these lines, we set up a series of experiments in which micro- and macro-objects were placed in an aqueous environment. For instance, in the case of the micropillar array of Fig. 4 (A and B), the membrane envelops the underlying micropattern, producing a peak-and-valley–shaped polymer film with arrayed bumps. The deformation of the polymer membrane appears evident even in the case of a little cluster of latex microparticles. The SEM images of Fig. 4C show the polymer enveloping of five microspheres and the wrinkling arising in close contact with the surface. The presence of the membrane is also revealed by the level of gray color, more evident if compared to the corresponding group of noncoated microspheres. The fabrication of PLGA membranes even works on a 3D macroarray, for example, in Fig. 4 (D and E), a drop of polymer is dispensed over a matrix of microspheres submerged in water. The resulting film is formed over the macroarray in a semi–free-standing modality with a profile following the underlying geometry. The wrinkle formation on the 3D structures could be explained considering the equation balance of the forces acting on the polymer film taking into account the solvent evaporation rate, as illustrated detail in Supplementary Text 2 and fig. S4. These additional functionalities would be crucial for the design of cell culturing substrates, scaffolds for tissue engineering, and drug delivery systems where the drugs of interest could be delivered controlling the material properties (they could be embedded directly into the polymer or could be enveloped by the membrane) (*10*, *11*). Moreover, the growing interest for a novel sensing platform for in situ and real-time experiments could lead to the application of the method proposed for the fabrication of a polymer membrane directly over optical fibers. Biochemical sensing typically requires that optical signal interacts with the external media, either directly with a given analyte or through the measurement of the refractive index of an auxiliary membrane. The fabrication technique discussed could be implemented for the design of polymeric coating on optical fibers for sensing application (*37*, *38*). Depending on the location of the sensitive coating along the optical fiber, many different architectures can be found. Reflection (rx) and transmission (tx) configurations can be used to exploit different optical phenomena such as optical absorbance, fluorescence, or evanescent field (Ef) (*39*). The polymer coating, as shown in Fig. 4F, could provide an attractive solution for the design and fabrication of a sensitive layer in close contact with the fiber surface. As a consequence of the configuration selected, the membrane could cover the end of the fiber tip (rx) and the external cylindrical surface of the clad (tx) or could be fabricated directly on the core (Ef). In this case, the fiber was dipped in water and the packaging was performed before the evaporation takes place, avoiding the formation of wrinkles on the area of interest; the coating layer appears uniform and smooth with a thickness comparable with the mean value reported in the characterization

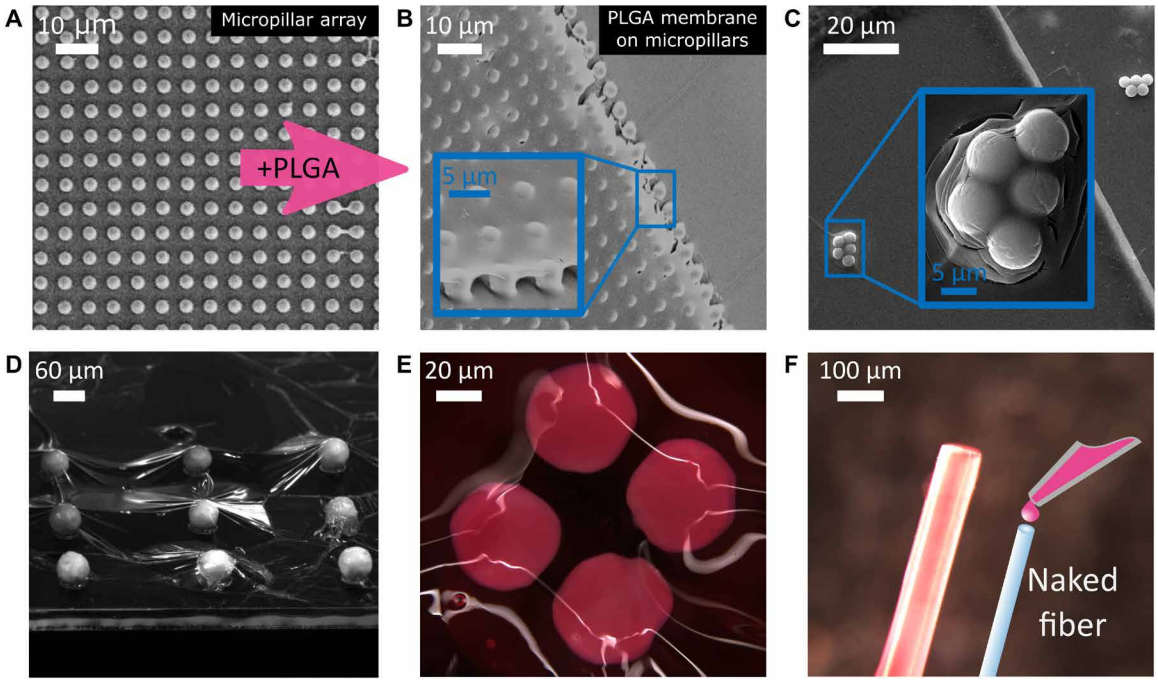

Fig. 4. Polymer packaging of micropillars, macroarray, and optical fiber. (**A**) SEM image of micropillar array (top view) and (**B**) corresponding SEM image of polymer membranes suspended over the micropillar structure. (**C**) Packaging of five latex microspheres. The difference between coated (left) and uncoated (right) microspheres is evident. (**D** and **E**) Side view and top view of water packaging for a matrix of microspheres submerged in water. (**F**) Outline of polymer membrane formation directly onto the top of optical fiber and stereoscope image of the coating realized.

section. The opportunity of producing the polymer film onto a supporting substrate from which it could be simply peeled off and then moved on different targets would increase its feasibility of use.

Hydrogels as stamps for polymer membranes

Hydrogels could be used for surface packaging as stamps for polymeric film formation with easily peeling properties because of the weak forces at the interface acting between the polymer and the gel surface. Hydrogel elements were chosen as templates because of their high water content. A polymer drop is simply dispensed (Fig. 5A) or sprayed (Fig. 5B) over a rotating hydrogel cylinder, resulting in the formation of a continuous polymer film. Because the PLGA solution completely wets the hydrogel surface, the generated interfacial tensions largely surpass the cohesive forces or dissipations due to viscous flow and limit the spreading of polymer wrinkling. The images reported in Fig. 5 (C and D) show the possibility of using hydrogels as stamps for producing uniform and regular polymer films into different molds: microcube, rhombus, and cylinder. However, a problem related to the method of fabrication would be the identification of the influence of geometry and the interfacial effects over the process. To bypass this limitation, we tested the possibility of producing a thin polymer film held up over metal tips as shown in Fig. 5 (E and F). In this case, we studied the fabrication of packaging onto an ordered micropillar array. From a technological point of view, the film is suspended over the pillar array, and it would be possible to study its properties confining the interfacial effects and removing the contact effects with an attractive surface, as usually happens (*40*). The preparation of a polymer film often requires a method based on the presence of a substrate (spin coating, blade coating, drop casting, etc.) while, in the case of water, once the film of interest is prepared, it would be just necessary to pick up the film from the water, transferring onto the desired setup of analysis. The image shown in Fig. 5F makes also visible the light convexity of the polymer tent as evidence of the preexisting underlying water pool; during the evaporation, the membrane crouches in the middle region held up by the metallic pins. In Fig. 5G, it is proposed that as an additional functionality, a needle could be inserted before the packaging takes place to create a membrane with a "passageway" for promoting the mix-up or the exchange of substances between the two adjacent layers, the liquid below the membrane and the upper one.

Controlling cell-material interactions on polymer membranes

The use of hydrogel elements coated with a biopolymer membrane could become a key component for the bottom-up tissue engineering approach in which the cells self-assemble together with instructive engineered micro-objects (*9*). Hydrogels could be used as scaffolding elements so that the compaction and morphology of the formed tissue construct could be modulated with well-established properties including spatial and temporal control at the cellular level. To validate the use of the proposed packaging approach and to demonstrate that our method did not harm cell cultures, we performed preliminary experiments regarding the growth of cells over 3D membranes obtained by packaging hydrogels of various shapes: macrospheres, cubes, and polymer patterns (Fig. 6). We analyzed the morphological features of human mesenchymal stem cells (hMSCs) seeded on top of the PLGA membranes and over the peak and valley membrane surface produced onto a matrix of micropillars, cultivated for 24 hours, and then fixed and stained for the visualization of cytoskeletal stress fibers and nuclei (see Materials and Methods). Cell

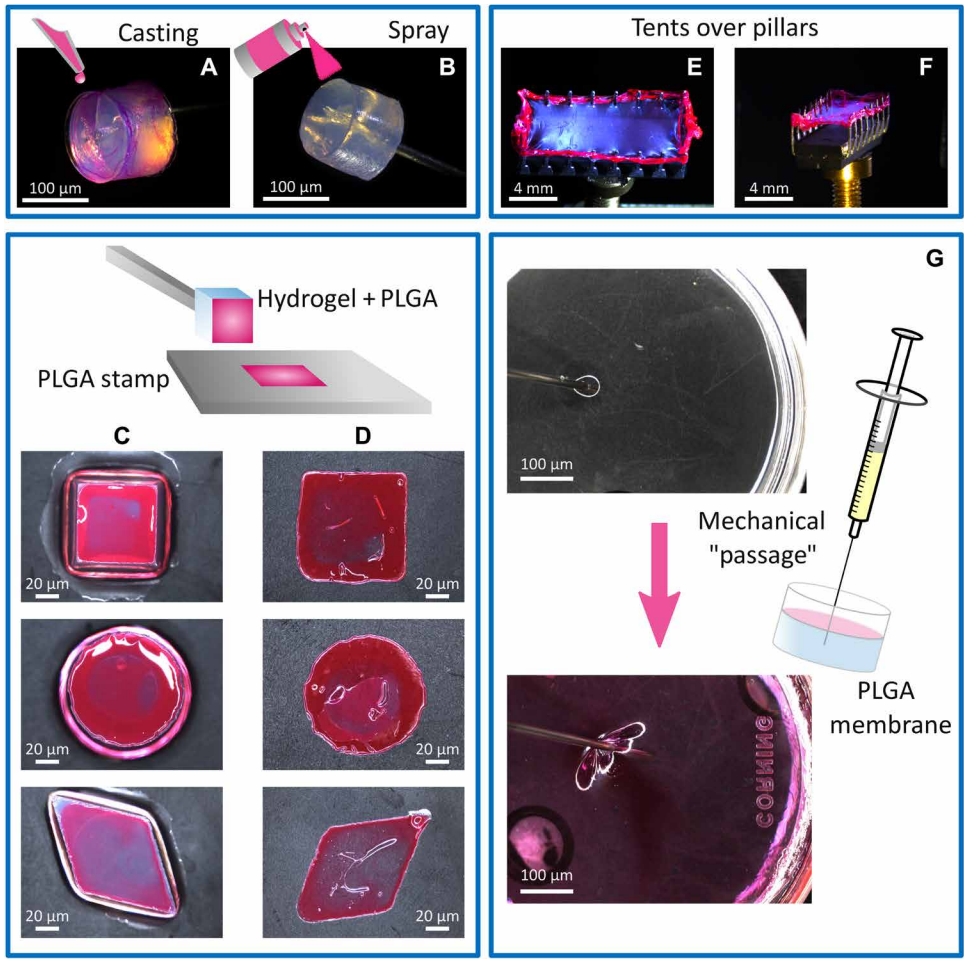

Fig. 5. Hydrogels as stamps for polymer membranes. Formation of the polymer film on a rotating cylinder hydrogel by dispensing (**A**) or spraying (**B**). Scale bars, 100 μm. Regular-shaped membranes fabricated over a hydrogel face (**C**) can be easily peeled off and placed over any substrates (**D**). Scale bars, 20 μm. A suspended PLGA membrane over an array of micropillars (**E** and **F**) Tents are used to study the behavior of the membrane's formation process, avoiding the influence of interfacial and contact effects. In (**G**), simply using a needle, we are able to produce a passage between "inside" and "outside" the membrane and, at the same time, to produce wrinkles mechanically induced.

bodies were predominantly elongated over the polymer film (Fig. 6, A to C). The results showed that the polymer film produced by water packaging is a safe and good tool for designing arbitrary and complex microarchitectures with a mold-free approach. As a consequence, the proposed fabrication process appears not to harm cell cultures or microorganisms, opening the way to a 3D approach based on hydrogels used just as supporters or stamps of 3D membranes. The proposed technique starts from a very simple way to fabricate films that could be easily scaled up to generate the framework for microfluidic organ-on-chip technology.

DISCUSSION

In summary, we have developed an environment-friendly, cost-effective water-based bottom-up approach in which we let a biopolymer self-assemble over the water surface and over 3D liquid templates. The method is also effective under dynamic conditions and against the gravity force, making the isolation and packaging of temporary and unstable liquid shapes possible. Once produced, the polymer film could be collected from the water as a free-standing membrane and transferred directly to the device of interest. Moreover, the self-adaptable polymeric film wrapping could be used as a natural layer for in vitro lab-in-a-drop experiments and in vivo indwelling devices that could find application in a clinic as an injectable system or for the creation of biomimetic materials that can be integrated into living organisms. We demonstrated the effectiveness and performance of the method with a sequence of experiments involving coating/encapsulating inorganic or organic objects and microstructured surfaces. The range of applications spans from biotechnology and biomedicine to wound care applications and organ-on-chip technology. Micropatterning of the film surface would be used to control cell behavior, whereas, the addition of chemical components could add antimicrobial activity, making the film more resistant to bacterial attachment. Overall, the possibility of encasing and packaging water in microcontainers could open a new route for microgravity experiments of biotechnology, materials science, and fluid dynamics. Functionalization of polymeric film with semiconductor nanoparticles, or quantum dots, could open new routes for clinical phototherapy in living systems.

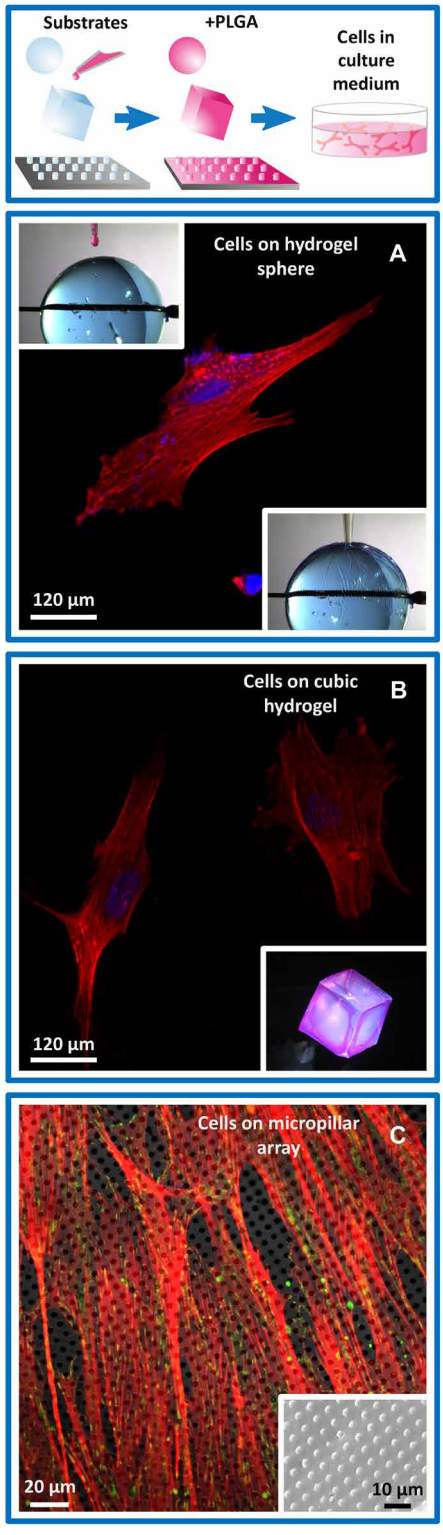

Fig. 6. Controlling cell-material interactions on polymer membranes. Schematic overview of polymer membranes onto different shaped hydrogels and cells growing over them: (**A**) sphere, (**B**) cube, and (**C**) micropillar matrix. Digital images of actin filaments and focal adhesion were collected with an LSM ConfoCor 710 (Zeiss). Tetramethyl rhodamine isothiocyanate (TRITC)–phalloidin–conjugated actin fibers were excited with a 543-nm He-Ne laser, and emitted radiation was collected in the 560- to 600-nm interval.

MATERIALS AND METHODS

Polymeric solution

PLGA 50:50 (38,000 to 54,000 Da; PLGA Resomer RG 504H, Boeringer Ingelheim) was dissolved in DMC [20 to 30 (w/v); DMC, 99%; Sigma-Aldrich).

Membrane preparation

The fabrication of the polymeric membranes used for the characterization was performed using a solution of PLGA in DMC [25% (w/w)]. A solution drop of 20 µl was delivered in a petri dish (diameter, 100 mm; height, 15 mm) filled with water. Polyethylene terephthalate masks were placed at the bottom of the petri dish and completely submerged in water. These masks were realized as a sort of frame, with the dimension and the shape needed for the slot for the sample's positioning required by the instrument involved in the process of characterization. Once the solution droplet was dispensed over the water surface, the polymer membrane was formed floating on the water surface, and it was finally picked up using the polyethylene terephthalate (PET) frame. We waited 24 hours at ambient temperature for complete water evaporation, to remove small water droplets eventually present on the membrane. Once the polymer membrane was completely dry, it was placed in the sample's slot and the external frame was removed to characterize the membrane's properties.

Membrane characterization

PLGA surfaces and cross sections were observed through SEM by means of a Quanta 200 FEG SEM (FEI, Eindhoven, The Netherlands) in a high-vacuum mode. Before SEM observations, membrane samples were mounted onto SEM stubs by means of carbon adhesive disks and sputter-coated with a 5- to 10-nm-thick Au-Pd layer. All the samples were observed at 10- to 20-kV acceleration voltage using a secondary electron detector.

An FTA 1000 (First Ten Ångstroms, Portsmouth, VA, USA) instrument was used to measure static CAs of the PLGA membrane. A 1-µl distilled water droplet was positioned on the film surface. The experiments were conducted at RT. CA values were geometrically evaluated as the angle formed by the solid surface and the tangent to the droplet. The measurement was repeated four times, calculating the average CA value and the SD.

The UV-visible spectrum of a PLGA membrane (thickness, about 1.5 µm) was collected on a V-570 UV spectrophotometer (Jasco, Easton, PA, USA) in the 200- to 800-nm wavelength range and with 0.5-nm resolution.

Tensile tests were performed on rectangular-shaped samples (thickness, about 1.5 µm; width, 6 mm; gauge length, 10 mm) of PLGA membranes on a microtensile test apparatus (Deben, Woolpit, UK). Stress strain curves were recorded at 25° ± 1°C and 50 ± 5% relative humidity (RH) with a 200 N load cell and a crosshead speed of 0.1 mm/min.

Water vapor and oxygen permeability were evaluated by means of a Multiperm apparatus (ExtraSolution, Pisa, Italy) working in a gas/membrane/gas configuration. The exposed area of the film was 2.0 cm^2. Measurements were performed at 25° ± 1°C and 50 ± 0.5% RH.

Cell cultures

hMSCs were purchased from Lonza. hMSCs were cultured in α-MEM (α–modified Eagle's medium; BioWhittaker) supplemented with 10% fetal bovine serum (Thermo Fisher Scientific), L-glutamine

(100 mg/ml), and penicillin/streptomycin (100 U/ml; Sigma-Aldrich). hMSCs were kept in a humidified atmosphere at 37°C and 5% CO_2. The medium was replaced every 3 days. hMSCs were used at passage 4, were detached from the cell culture flasks with trypsin/EDTA [0.25% (w/v) trypsin/0.02 mM EDTA] (Sigma-Aldrich), and seeded on PLGA-coated hydrogels at the density of 103 cells/cm^2.

Actin filaments and nuclei were visualized with confocal microscopy. Briefly, after 24 hours from the seeding procedure, cells cultured on PLGA-coated hydrogels were fixed in 4% paraformaldehyde (Sigma-Aldrich) for 20 min at RT, and then, the samples were washed with PBS and incubated with 0.1% PBS–Triton X-100 (Sigma-Aldrich) solution. After 5 min at RT, the PLGA-coated hydrogels were rinsed twice with PBS. Actin filaments were stained with TRITC-conjugated phalloidin (dilution, 1:200; Sigma-Aldrich) for 30 min at RT.Cell nuclei were stained by incubating samples with 4′,6-diamidino-2-phenylindole (1:1000 in PBS) for 15 min at RT.

Digital images of actin filaments and focal adhesion were collected with an LSM ConfoCor 710 (Zeiss). TRITC-phalloidin–conjugated actin fibers were excited with a 543-nm He-Ne laser, and emitted radiation was collected in the 560- to 600-nm interval.

Agarose gels

Agarose gels were prepared by dissolving 1 g of type I agarose (Sigma-Aldrich) in 100 ml of bidistilled water. The solution was then autoclaved for 30 min. Agarose solution gelified quickly at RT; therefore, stock gels were first melted in a microwave oven at 500 W for 30 s. To produce cubic or cylindric hydrogels, hot agarose solutions were poured in polyethylene molds, which were then placed in a 4°C fridge for 2 hours. Molds containing hydrogels were rinsed in abundant water at RT, and the hydrogels were gently detached from the molds with a spatula. Hydrogel spheres were produced by dripping hot agarose solution from a 10-ml plastic syringe in an ice-cold water bath, thus obtaining 3-mm spheres.

SUPPLEMENTARY MATERIALS

Supplementary material for this article is available at http://advances.sciencemag.org/cgi/content/full/5/5/eaat5189/DC1

Supplementary Text 1. Encasing 3D silhouettes

Supplementary Text 2. Wrinkles

Fig. S1. SEM image of a collapsed membrane on microscale sessile drop.

Fig. S2. Complete encasing and wrapping of a 3D hydrogel sphere.

Fig. S3. Image of a wrapped and detached liquid bridge.

Fig. S4. Wrinkling formation on the free water surface.

Movie S1. Water packaging of a sessile drop.

Movie S2. Slippery test with and without the PLGA membrane.

Movie S3. Induced paralysis by polymer packaging of *C. elegans*.

Movie S4. *C. elegans* after removing the membrane.

References (*41*–*52*)

REFERENCES AND NOTES

1. P. M. Wilson, A. Zobel, A. Lipatov, E. Schubert, T. Hofmann, A. Sinitskii, Multilayer graphitic coatings for thermal stabilization of metallic nanostructures. *ACS Appl. Mater. Interfaces* **7**, 2987–2992 (2015).
2. R. H. Muller, K. Mäder, S. Gohla, Solid lipid nanoparticles (SLN) for controlled drug delivery — A review of the state of the art. *Eur. J. Pharm. Biopharm.* **50**, 161–177 (2000).
3. B. Sobrino, M. Bríon, A. Carracedo, SNPs in forensic genetics: A review on SNP typing methodologies. *Forensic Sci. Int.* **154**, 181–194 (2005).
4. A. Y. Romanchuk, A. S. Slesarev, S. N. Kalmykov, D. V. Kosynkin, J. M. Tour, Graphene oxide for effective radionuclide removal. *Phys. Chem. Chem. Phys.* **15**, 2321–2327 (2013).
5. A. Marino, C. Filippeschi, V. Mattoli, B. Mazzolai, G. Ciofani, Biomimicry at the nanoscale: Current research and perspectives of two-photon polymerization. *Nanoscale* **7**, 2841–2850 (2015).
6. L. Persano, A. Camposeo, D. Pisignano, Integrated bottom-up and top-down soft lithographies and microfabrication approaches to multifunctional polymers. *J. Mater. Chem.* **1**, 7663–7680 (2013).
7. D. Losic, J. G. Mitchell, R. Lal, N. H. Voelcker, Rapid fabrication of micro- and nanoscale patterns by replica molding from diatom biosilica. *Adv. Funct. Mater.* **17**, 2439–2446 (2007).
8. L. Ionov, Soft microorigami: Self-folding polymer films. *Soft Matter* **7**, 6786–6791 (2011).
9. A. Leferink, D. Schipper, E. Arts, E. Vrij, N. Rivron, M. Karperien, K. Mittmann, C. van Blitterswijk, L. Moroni, R. Truckenmuller, Engineered micro-objects as scaffolding elements in cellular building blocks for bottom-up tissue engineering Approaches. *Adv. Mater.* **26**, 2592–2599 (2014).
10. D. H. Gracias, J. Tien, T. L. Breen, C. Hsu, G. M. Whitesides, Forming electrical networks in three dimensions by self-assembly. *Science* **289**, 1170–1172 (2000).
11. M. Jamal, N. Bassik, J. H. Cho, C. L. Randall, D. H. Gracias, Directed growth of fibroblasts into three dimensional micropatterned geometries via self-assembling scaffolds. *Biomaterials* **31**, 1683–1690 (2010).
12. S. Schwaiger, M. Bröll, A. Krohn, A. Stemmann, C. Heyn, Y. Stark, D. Stickler, D. Heitmann, S. Mendach, Rolled-up three-dimensional metamaterials with a tunable plasma frequency in the visible regime. *Phys. Rev. Lett.* **102**, 163903–163904 (2009).
13. C. Moraes, B. C. Kim, X. Zhu, K. L. Mills, A. R. Dixon, M. D. Thouless, S. Takayama, Defined topologically-complex protein matrices to manipulate cell shape via three-dimensional fiber-like patterns. *Lab Chip* **14**, 2191–2201 (2014).
14. H. Clevers, Stem cells, asymmetric division and cancer. *Nat. Genet.* **37**, 1027–1028 (2005).
15. T. Leong, Z. Y. Gu, T. Koh, D. H. Gracias, Spatially controlled chemistry using remotely guided nanoliter scale containers. *J. Am. Chem. Soc.* **128**, 11336–11337 (2006).
16. A. Yulaev, A. Lipatov, A. X. Lu, A. Sinitskii, M. S. Leite, A. Kolmakov, Imaging and analysis of encapsulated objects through self-assembled electron and optically transparent graphene oxide membranes. *Adv. Mater. Interfaces* **4**, 1600734 (2016).
17. H. H. Wickman, J. N. Korley, Colloid crystal self-organization and dynamics at the air/water interface. *Nature* **393**, 445–447 (1998).
18. S. Grilli, S. Coppola, V. Vespini, F. Merola, A. Finizio, P. Ferraro, 3D lithography by rapid curing of the liquid instabilities at nanoscale. *PNAS* **37**, 15106–15111 (2011).
19. S. Coppola, G. Nasti, V. Vespini, V. Marchesano, P. Ferraro, On the spraying modality of liquids by pyroelectrohydrodynamics. *ACS Omega* **3**, 17707–17716 (2017).
20. S. Coppola, G. Nasti, M. Todino, F. Olivieri, V. Vespini, P. Ferraro, Direct writing of microfluidic footpaths by pyro-EHD printing. *ACS Appl. Mater. Interfaces* **9**, 16488–16494 (2017).
21. S. Coppola, V. Vespini, F. Olivieri, G. Nasti, M. Todino, B. Mandracchia, V. Pagliarulo, P. Ferraro, Direct self-assembling and patterning of semiconductor quantum dots on transferable elastomer layer. *Appl. Surf. Sci.* **399**, 160–166 (2017).
22. K. Shuto, Y. Oishi, T. Kajyama, C. C. Han, Preparation of 2-dimensional ultra thin polystyrene film by water casting method. *Polym. J.* **25**, 291–300 (1993).
23. D. Kumar, J. D. Paulsen, T. P. Russell, N. Menon, Wrapping with a splash: High-speed encapsulation with ultrathin sheets. *Science* **359**, 775–778 (2018).
24. N. Bremond, E. Santanach-Carreras, L. Y. Chu, J. Bibette, Formation of liquid-core capsules having a thin hydrogel membrane: Liquid pearls. *Soft Matter* **6**, 2484–2488 (2010).
25. A. Roointan, S. Kianpour, F. Memari, M. Gandomani, S. M. G. Hayat, S. Mohammadi-Samani, Poly(lactic-co-glycolic acid): The most ardent and flexible candidate in biomedicine! *Int. J. Polym. Mater. Polym. Biomater.* **67**, 1028–1049 (2018).
26. T. Schleeh, G. Hinrichsen, G. Kossmehl, Spontaneous film formation from a polymer-solution. *Colloid Polym. Sci.* **270**, 207–211 (1992).
27. G. R. Guillen, Y. J. Pan, M. H. Li, E. M. V. Hoek, Preparation and characterization of membranes formed by nonsolvent induced phase separation: A review. *Ind. Eng. Chem. Res.* **50**, 3798–3817 (2011).
28. N. T. Paragkumar, E. Dellacherie, J.-L. Six, Surface characteristics of PLA and PLGA films. *Appl. Surf. Sci.* **253**, 2758–2764 (2006).
29. S. Zanini, C. Riccardi, A. Natalello, G. Cappelletti, D. Cartelli, F. Fenili, A. Manfredi, E. Ranucci, Covalent immobilization of bioactive poly(amidoamine)s onto plasma-functionalized PLGA surfaces. *Mater. Res. Express* **1**, 035001 (2014).
30. Y. Liu, Y. Yin, L. Y. Wang, W. F. Zhang, X. M. Chen, X. X. Yang, J. J. Xu, G. H. Ma, Surface hydrophobicity of microparticles modulates adjuvanticity. *J. Mater. Chem. B* **1**, 3888–3896 (2013).
31. J. J. Park, E. J. Yu, W. K. Lee, C. S. Ha, Mechanical properties and degradation studies of poly(D,L-lactide-co-glycolide) 50:50/graphene oxide nanocomposite films. *Polym. Adv. Technol.* **25**, 48–54 (2014).
32. R. Avolio, R. Castaldo, G. Gentile, V. Ambrogi, S. Fiori, M. Avella, M. Cocca, Plasticization of poly(lactic acid) through blending with oligomers of lactic acid: Effect of the physical aging on properties. *Eur. Polym. J.* **66**, 533–542 (2015).
33. J. Wang, D. J. Gardner, N. M. Stark, D. W. Bousfield, M. Tajvidi, Z. Y. Cai, Moisture and oxygen barrier properties of cellulose nanomaterial-based films. *ACS Sustainable Chem. Eng.* **6**, 49–70 (2017).
34. R. Avolio, R. Castaldo, M. Avella, M. Cocca, G. Gentile, S. Fiori, M. E. Errico, PLA-based plasticized nanocomposites: Effect of polymer/plasticizer/filler interactions on the time evolution of properties. *Compos. Part B Eng.* **152**, 267–274 (2018).

35. A. Albeg, C. J. Smith, M. Chatzigeorgiou, D. G. Feitelson, D. H. Hall, W. R. Schafer, D. M. Miller, M. Treinin, C-elegans multi-dendritic sensory neurons: Morphology and function. *Mol. Cell. Neuroci.* **46**, 308–317 (2011).
36. R. Nass, K. M. Merchant, T. Ryan, Caenorhabditis elegans in Parkinson's disease drug discovery: Addressing an unmet medical need. *Mol. Interv.* **8**, 284–293 (2008).
37. D. K. Chow, C. F. Glenn, J. L. Johnston, I. G. Goldberg, C. A. Wolkow, Sarcopenia in the Caenorhabditis elegans pharynx correlates with muscle contraction rate over lifespan. *Exp. Gerontol.* **41**, 252–260 (2006).
38. A. Cusano, M. Consales, A. Crescitelli, A. Ricciardi, *Lab-On-Fiber Technology* (Springer Series in Surface Sciences, Springer International Publishing, 2015).
39. P. J. Rivero, J. Goicoechea, F. J. Arregui, Optical fiber sensors based on polymeric sensitive coatings. *Polymers* **10**, E280 (2018).
40. M. Campoy-Quiles, T. Ferenczi, T. Agostinelli, P. G. Etchegoin, Y. Kim, T. D. Anthopoulos, P. N. Stavrinou, D. D. C. Bradley, J. Nelson, Morphology evolution via self-organization and lateral and vertical diffusion in polymer: Fullerene solar cell blends. *Nat. Mater.* **7**, 158–164 (2008).
41. T. A. Witten, Stress focusing in elastic sheets. *Rev. Mod. Phys.* **79**, 643–675 (2007).
42. J. W. S. Rayleigh, *The Theory of Sound* (Dover, 2007), vol. 1, pp. 19–20.
43. R. D. Schroll, M. Adda-Bedia, E. Cerda, J. Huang, N. Menon, T. P. Russell, K. B. Toga, D. Vella, B. Davidovitch, Capillary deformations of bendable films. *Phys. Rev. Lett.* **111**, 014301–014305 (2013).
44. E. Cerda, L. Mahadevan, Geometry and physics of wrinkling. *Phys. Rev. Lett.* **90**, 074302 (2003).
45. L. Pocivavsek, B. Leahy, N. Holten-Andersen, B. Lin, K. Y. C. Lee, E. Cerda, Geometric tools for complex interfaces: From lung surfactant to the mussel byssus. *Soft Matter* **5**, 1963–1968 (2009).
46. H. King, R. D. Schroll, B. Davidovitch, N. Menon, Elastic sheet on a liquid drop reveals wrinkling and crumpling as distinct symmetry-breaking instabilities. *Proc. Natl. Acad. Sci. U.S.A.* **109**, 9716–9720 (2012).
47. G. M. Grason, B. Davidovitch, Universal collapse of stress and wrinkle-to-scar transition in spherically confined crystalline sheets. *Proc. Natl. Acad. Sci. U.S.A.* **110**, 12893–12898 (2013).
48. E. Hohlfeld, B. Davidovitch, Sheet on a deformable sphere: Wrinkle patterns suppress curvature-induced delamination. *Phys. Rev. E* **91**, 012407 (2015).
49. D. Vella, J. Huang, N. Menon, T. P. Russell, B. Davidovitch, Indentation of ultrathin elastic films and the emergence of asymptotic isometry. *Phys. Rev. E* **114**, 014301 (2015).
50. L. D. Landau, E. M. Lifshitz, *Theory of Elasticity* (Pergamon Press, 1986).
51. J. D. Paulsen, E. Hohlfeld, H. King, J. S. Huang, Z. L. Qiu, T. P. Russell, N. Menon, D. Vella, B. Davidovitch, Curvature-induced stiffness and the spatial variation of wavelength in wrinkled sheets. *PNAS* **113**, 1144–1149 (2016).
52. Z. Y. Huang, W. Hong, Z. Suo, Nonlinear analyses of wrinkles in a film bonded to a compliant substrate. *J. Mech. Phys. Solids* **53**, 2101–2118 (2005).

Acknowledgments: We thank M. Iannone, E. di Schiavi, and V. Marchesano for supporting the experiments on cells and *C. elegans*. We thank A. Finizio for the fluorescence images of the 3D membranes acquired with technical and artistic expertise. **Funding:** We acknowledge financial support from the project PM3-Piattaforma Modulare Multi-Missione under the National Research Program PON 2014-2020 (ARS01_01181). **Author contributions:** S.C. and P.F. designed the experiments of water encasing. P.F. and P.A.N. convinced the experiments on 3D hydrogels. S.C., G.N., V.V., and L.M. conducted the experiments of water packaging of temporary 3D silhouettes, sessile droplets, and micro-objects. S.C. and L.M. performed the experiments with *C. elegans*. S.C., P.F., and G.N. scored the experimental data. G.G. and R.C. conducted the characterization of the membranes produced. M.V. and P.A.N. studied cell-material interactions on polymer membranes. S.C. and P.F. performed the analyses and wrote the paper with contributions from all authors. **Competing interests:** The authors declare that they have no competing interests. **Data and materials availability:** All data needed to evaluate the conclusions in the paper are present in the paper and/or the Supplementary Materials. Additional data related to this paper may be requested from the authors.

Submitted 9 March 2018
Accepted 17 April 2019
Published 24 May 2019
10.1126/sciadv.aat5189

Citation: S. Coppola, G. Nasti, V. Vespini, L. Mecozzi, R. Castaldo, G. Gentile, M. Ventre, P. A. Netti, P. Ferraro, Quick liquid packaging: Encasing water silhouettes by three-dimensional polymer membranes. *Sci. Adv.* **5**, eaat5189 (2019).

ScienceAdvances

Quick liquid packaging: Encasing water silhouettes by three-dimensional polymer membranes

Sara Coppola, Giuseppe Nasti, Veronica Vespini, Laura Mecozzi, Rachele Castaldo, Gennaro Gentile, Maurizio Ventre, Paolo A. Netti and Pietro Ferraro

Sci Adv **5** (5), eaat5189.
DOI: 10.1126/sciadv.aat5189